Environmental Science & Technology

Article

pubs.acs.org/est

Assessment of Estrogenic Activity of Perfluoroalkyl Acids Based on Ligand-induced Conformation State of Human Estrogen Receptor

Yu Gao, Xinxin Li, and Liang-Hong Guo*

State Key Laboratory of Environmental Chemistry and Ecotoxicology, Research Center for Eco-Environmental Sciences, Chinese Academy of Sciences, P.O. Box 2871, 18 Shuangqing Road, Beijing 100085, China

Supporting Information

ABSTRACT: Perfluoroalkyl acids (PFAAs) have been reported to interfere with the endocrine system in vivo by mimicking endogenous hormone activities and causing adverse effects. Some exoestrogens bind to estrogen receptor (ER) and subsequently induce an ER-mediated response. The transcriptional activity of ER is regulated by its distinct conformational states that are the results of ligand binding. In this work, a biosensor based on surface plasmon resonance (SPR) technique was developed which can discriminate between agonist and antagonist of human ERα (hERα) by monitoring the conformation state of the protein induced by ligand binding. The biosensor utilized the specific interaction between hERα and conformation-selective peptides. Six PFAAs with different chain lengths and acid groups were tested by the biosensor, and perfluorooctane sulfonate (PFOS) and perfluorooctanoic acid (PFOA) were found to be ER agonists. Kinetic analyses of direct interaction between PFAAs and hERα by SPR revealed that PFOS and PFOA were both weak binders of ER with K_D values of 2.19 and 107 μM respectively, whereas the other four PFAAs did not bind with ER. To understand the differences in ER binding affinity and estrogenic activity among the six PFAAs, molecular docking based on the crystal structure of hERα ligand binding domain was performed. PFOS and PFOA were efficiently docked with hERα and formed hydrogen bonds with Arg394 in a manner similar to estradiol. Overall, the two 8-carbon PFAAs were assessed as weak agonists of hERα and are of potential concern.

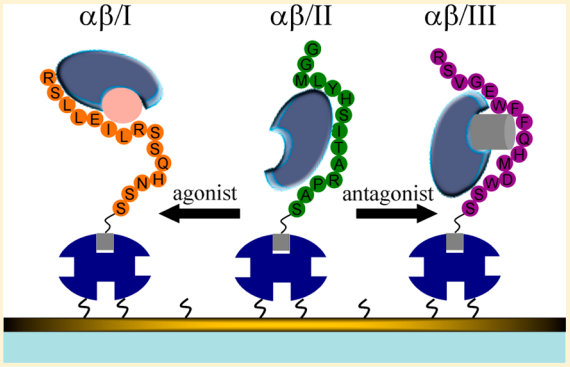

INTRODUCTION

Perfluoroalkyl acids (PFAAs) are a family of fluorine-containing chemicals with unique properties including repellency to oil, stain, grease, and water, as well as fire resistance, which render them many industrial and commercial applications. According to the documents submitted to the Stockholm Convention Persistent Organic Pollutants Review Committee by 3 M Company, the global production of perfluorooctane sulfonate (PFOS) was 3500 t in 2000, and that of perfluorooctanoic acid (PFOA) was estimated at 500 t per year.[1] PFAAs have been found to be widespread in the environment, and accumulate in wildlife and humans.[2−4] A number of studies have demonstrated the adverse effects of PFAAs on experimental animals, mostly of PFOA and PFOS.[5] Consequently, regulators have begun to take actions to limit the production and consumption of PFAAs. The U.S. Environmental Protection Agency initiated the PFOA Stewardship Program in 2006 with an aim to reduce facility emissions and product contents of PFOA and related chemicals. In 2009, PFOS was added to the list of persistent organic pollutants of the Stockholm Convention to reduce and eventually eliminate its production and use. However, due to their persistence, bioaccumulation and biomagnification through the food chain,[6] the environmental behavior and the risk to human health of PFAAs are still worthy of long-term concern.

The toxicity of PFAAs has been investigated extensively in the past decade or so, which includes loss of body weight, hepatotoxicity, interference of lipid transportation and metabolism, endocrine effects, tumorigenicity and developmental toxicity.[7] Due to their structure similarity to fatty acids, early studies focused on the toxicity mechanisms involving ligand-dependent activation of the hepatic peroxisome proliferator receptor α (PPARα), which induces enzymes responsible for β-oxidation, fatty acid ω-oxidation and cholesterol homeostasis.[8,9] In vitro competitive binding of PFAAs with serum albumin (a transport protein) was also evaluated as a possible route of disruption on fatty acid transport in blood.[10,11] More recently, increasing attention has been paid to the role of estrogenic activity of PFAAs in their hepatocarcinogenesis due to the observation of increased liver cancer incidence by PFAAs in PPARα knockout mice.[12,13] Genomic profiling of rainbow trout (an animal model insensitive to peroxisome proliferation) exposed to PFOA revealed possible mechanisms involving estrogenic signaling.[14] Estrogenic activities of selected perfluorinated chemicals were investigated using vitellogenin

Received: October 5, 2012
Revised: November 30, 2012
Accepted: December 7, 2012
Published: December 7, 2012

ACS Publications © 2012 American Chemical Society

dx.doi.org/10.1021/es304030x | Environ. Sci. Technol. 2013, 47, 634−641

(VTG, an estrogen responsive biomarker) induction in primary cultured tilapia hepatocytes. A dose-dependent induction of VTG was observed in PFOS- and PFOA-treated cells.[15] However, an in vitro yeast two-hybrid assay found no interaction between medaka estrogen receptor and coactivator after treatment with any of the five PFAAs including PFOS and PFOA.[16] Using VTG induction in rainbow trout, trout ER competitive binding assay and human ERα gene reporter assay, a number of PFAAs with different chain length and acid groups were investigated for their estrogenic activity. Several PFAAs including PFOS and PFOA were assessed to be weak environmental xenoestrogens.[17] Putting together, these different results indicate that the estrogenic effect of PFAAs may depend on the animal species and route of exposure. Consequently, a mechanistic study on the interactions between PFAAs and hERα at molecular level is highly desired. In addition to estrogenic effect, several studies also found depression of thyroid hormone levels in PFOS-exposed rats,[18,19] and interactions of PFAAs with thyroid hormones transport proteins.[20]

Ligand binding induces distinct conformational alteration of the ER ligand binding domain (LBD), and then may trigger gene transcription and disturb the hormone response pathways.[21] It is reported that the specific conformation changes in the ER-LBD are highly dependent on the structure of the ligand. The crystal structure reveals that ER-LBD consists of 12 helixes, which form a three-layered antiparallel α-helical sandwich conformation. This arrangement creates a hydrophobic cavity at the narrow end of the domain, which can accommodate homologous ligand. When E2 (an agonist of ER) binds to ER, the helix 12 (H12) seals the ER ligand binding pocket (H3, H5/6, and H11) and generates a hydrophobic groove on the surface of LBD for binding LXXLL (where L is leucine and X is any amino acid) short peptide motifs found in many ER coactivators[22] However, in the complex of 4-OH tamoxifen (OHT, an antagonist of ER) and ER, H12 blocks the coactivator recognition groove by mimicking the interactions of nuclear receptor box peptide with LBD.[23] Meanwhile, both of the conformations described above are distinct to the unliganded ER (apo-ER). In 1999, McDonnell and colleagues identified peptides that interacted selectively with estradiol- or tamoxifen-activated ERα,[24] and found three peptide-probes for different ERα conformations (apo-ER, E2-ER, and OHT-ER). They also provided a strong correlation between ligand induced ER conformations and their biological activities.[25] Previous studies using piezoresistive cantilevers,[26] electrochemical sensor,[27] and reflectometric interference spectroscopy[28] have successfully detected the ligand induced ER conformation change through specific peptide-probes.

Surface plasmon resonance biosensors are widely used for the investigation of biological processes, especially for measuring directly the binding interactions between small molecules and proteins in real-time.[29] This label-free method (without radioactive or fluorescent probe) provides both kinetic and affinity information on ligand−receptor interactions, and avoids structural alteration by the labels.[30] Thus, this technique has become a central tool for characterizing and quantifying biomolecular interactions.

In the present work, an SPR-based sensor method was developed for the assessment of estrogenic effects of selected PFAAs. This method employs peptide probes to recognize ligand-induced ER conformation state which is indicative of estrogenic activity of the ligand. By combining with SPR-based direct ER binding assay and molecular docking, some structural characteristics of the estrogen-like PFAAs were identified.

EXPERIMENTAL SECTION

Chemicals. *N*-(3-dimethylaminopropy)-*N*′-ethylcarbodiimide hydrochloride (EDC), *N*-hydroxysuccinimide (NHS), 11-mercaptoundecanoic acid (MUA), 17β-estradiol (E2), 4-OH tamoxifen (OHT), perfluorobutyric acid (PFBA), perfluorobutane sulfonic acid (PFBS), perfluorooctanoic acid (PFOA), perfluorooctane sulfonic acid potassium salt (PFOS), perfluorododecanoic acid (PFDoDA), perfluorotetradecanoic acid (PFTeDA), and human serum albumin (HSA) were purchased from Sigma-Aldrich (St. Louis, MO). Ethanolamine hydrochloride was obtained from Alfa Aesar (Ward Hill, MA). Recombinant human estrogen receptor α (hERα) and GST-tagged hERα ligand binding domain (hER-LBD) were from Panvera Corp. (Madison, WI), and streptavidin (SA) was from Promega Corp. (Madison, WI). Anti-GST antibody (immunosorbent-purified polyclonal goat antibody) and recombinant GST were from GE Healthcare (Uppsala, Sweden). Biotinylated peptide $\alpha\beta$/I (SSNHQSSRLIELLSR), $\alpha\beta$/II (SAPRATISHYLMGG), and $\alpha\beta$/III (SSWDMHQFFWEGVSR) were purchased from GL Biochem Ltd. (Shanghai, China). All other reagents were acquired from general laboratory suppliers with analytical purity. Solutions were prepared in deionized water from a Millipore milli-Q (Biocel) water purification system (Billerica, MA).

Kinetic Analysis between hER-LBD and PFAAs. The kinetic analysis of six PFAAs with hER-LBD were performed on a Biacore 3000 instrument from GE Healthcare (Uppsala, Sweden) with a CM5 sensor chip. To immobilize ER, the sensor surface was first activated by NHS/EDC. A 30 μg/mL solution of anti-GST antibody was flown over the sensor for 4 min with HBS (10 mM HEPES, 0.15 M NaCl, pH 7.4) as running buffer. The remaining activated sites were blocked by flowing 1 M ethanolamine for 7 min. Recombinant GST of 5 μg/mL in HBS buffer was used to block the high affinity sites of anti-GST antibody that were difficult to regenerate. A 50 μL aliquot of GST-tagged hER-LBD (1.32 μM) was then injected into the flow cell, and was captured by the anti-GST antibody on the sensor surface. Finally, a ligand was injected into the flow cell while the SPR sensorgram was recorded. When necessary, the antibody surface was regenerated with 2 min injection of glycine-HCl (10 mM, pH 2.1). Triplicate measurements were performed for each ligand concentration. All data were double-referenced with blank injection and reference surface, and kinetic fitting was performed using the BIAevaluation software, Version 4.1 from the instrument manufacturer.

Preparation of Conformation-Specific Peptide Sensor Chip. Bare gold sensor chips (from Biosensing Instrument Inc., Tempe, AZ) were cleaned in Piranha solution (1:3 mixture of 30% hydrogen peroxide and concentrated sulfuric acid). The cleaned gold chips were immersed in a 4 mM MUA solution in ethanol for over 12 h. MUA-modified gold chips were loaded to the flow cell of a BI-SPR 1000 system (also from Biosensing Instrument Inc.). The chip surface was activated by injecting 50 μL mixture of 100 mM NHS and 400 mM EDC, using PBS as the running buffer. SA was immobilized on the activated surface by injecting 50 μL aliquot of 1 mg/mL protein into the flow cell. Residual activated sites were blocked by injection of 50 μL EA solution (1M). Finally, biotinylated peptide $\alpha\beta$/I, $\alpha\beta$/II, or

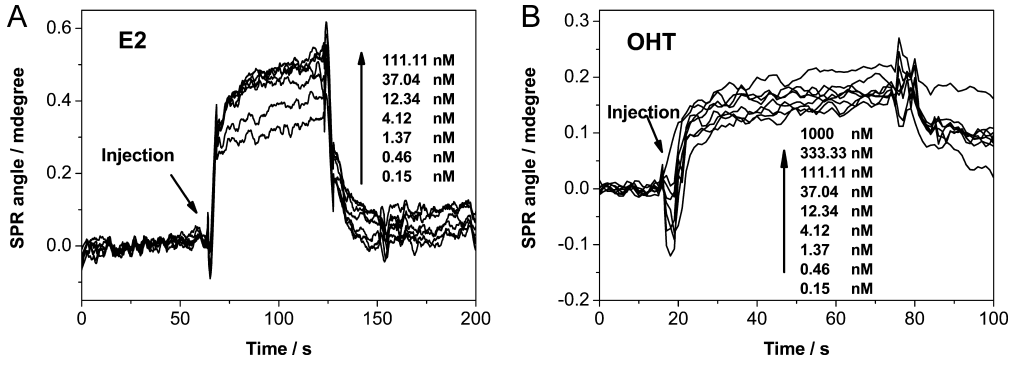

Figure 1. SPR sensorgrams of E2 (A) and OHT (B) binding with ER immobilized on the sensor chip. E2 was injected at a concentration of 0.15, 0.46, 1.37, 4.12, 12.34, 37.04, and 111.11 nM for 60 s, respectively; and OHT was injected at a concentration of 0.15, 0.46, 1.37, 4.12, 12.34, 37.04, 111.11, 333.33, and 1000 nM for 60 s, respectively.

$\alpha\beta$/III (1 mg/mL in PBS) was injected into the cell to form peptide sensor surface.

SPR Measurement of Ligand-Induced hERα Conformation State. All the ligands under investigation were dissolved in DMSO, yielding a 20 mM stock solution for each ligand. For SPR measurement, the stock solution was first diluted with DMSO into a series of concentrations, and then added into a hERα solution to yield a final concentration of 50 nM hERα. The ligand−receptor mixture was incubated at 25 °C for 90 min. After the SPR sensor surface was modified with a peptide, a 50 μL solution of the ligand−receptor mixture was injected into the flow cell at 10 μL/min, while SPR response was recorded. After each measurement, the peptide-modified chip surface was regenerated by injecting 50 μL of 0.1 M NaOH to remove surface-bound hERα. Triplicate measurements were performed for each ligand concentration.

Molecular Docking. The 3D crystal structure of hERα-LBD complexed with its antagonist OHT was obtained from the Protein Data Bank (PDB ID 3ERT).[23] PFAAs, E2, and OHT were docked to hERα-LBD using Lamarckian genetic algorithm provided by AutoDock 4.2 software.[31,32] Grid boxes were centered at the core of ER-LBD binding pocket and built around the protein with 60 × 60 × 60 points. A spacing of 0.375 Å between the grid points was used. Important docking parameters for the Lamarckian genetic algorithm included a population size of 150, maximum number of 2.5 million evaluations, maximum of 2700 generations, gene mutation rate of 0.02, crossover rate of 0.8, and 10 GA runs (each docking produced 10 docked conformations). Ten docked conformations for each ligand were scored according to a free energy cost function (ΔG^*) that accounted for Lennard-Jones and Coulomb electrostatic interactions, directional hydrogen bonding, an entropic contribution based on the loss of ligand conformational degree of freedom, and a desolvation term. The first ranked conformation of each ligand was selected for analysis and discussion.

RESULTS AND DISCUSSION

The aim of this work was to establish a SPR biosensor method for the monitoring of ligand-induced conformational change of ER, and to assess the estrogenic activity of the ligand based on ER conformational change. It is well-known that ligand binding to ER is the first and necessary step in ER mediated transcriptional activities. Therefore, direct binding of the ligands under study with ER was first investigated by SPR. In the experiment, ER was immobilized indirectly on a SPR sensor chip through an anti-GST antibody so as to maximize ER activity. A ligand of interest was then allowed to bind with ER on the sensor surface, and the SPR response was recorded in real time, as illustrated in Figure 1. From the sensorgram, k_a (association rate constant), k_d (dissociation rate constant), and K_D (equilibrium dissociation constant) values were obtained. E2 and OHT were tested as positive controls to validate the SPR method. The K_D value of E2 (0.31 nM) obtained in our assay is in good agreement with the results of fluorescence polarization (0.6 nM),[33] radio-labeled competitive assay (0.26 nM, 0.13 nM)[34,35] and SPR based assay (0.9 nM).[30] The K_D value of OHT (5.7 nM) is also within the range of 0.2−18 nM obtained by other reported methods.[30,36,37]

Several PFAAs with different chain lengths and acid groups were then measured. Ideally, one would select short-, medium-, and long-chain carboxylic acids and the corresponding sulfonic acids for structural comparison. However, commercially available perfluoroalkane sulfonates are very limited. As a result, six PFAAs, PFBA, PFBS, PFOA, PFOS, PFDoDA, and PFTeDA (see Figure S1 in the Supporting Materials for the structures) were selected for testing. All the values of k_a, k_d, and K_D of the tested PFAAs are listed in Table 1. Obviously, only

Table 1. Binding Affinity and Kinetic Constants between the Tested Ligands and hERα Determined by SPR[a]

ligand	k_a ($M^{-1}s^{-1}$)	k_d (s^{-1})	K_D (μM)	RBA (%)
E2	4.84×10^7	1.52×10^{-2}	0.000313	100
OHT	1.75×10^3	1.00×10^{-5}	0.00573	5.5
PFBA	nd	nd	nd	nd
PFBS	nd	nd	nd	nd
PFOA	6.73×10^2	7.23×10^{-2}	107	0.0003
PFOS	3.91×10^3	8.56×10^{-3}	2.19	0.014
PFDoDA	nd	nd	nd	nd
PFTeDA	nd	nd	nd	nd

[a] k_a, association rate constant; k_d, dissociation rate constant; K_D, equilibrium dissociation constant; RBA, relative binding Affinity; n.d., not determined.

the two 8-carbon perfluorinated compounds, PFOS and PFOA, were found by SPR to bind with ER, with a K_D value of 2.2 μM and 107 μM respectively. Compared to E2, PFOS and PFOA have much lower association rate constants (about 10^4 and 10^5 fold lower than E2), which result in weak affinity to hERα. The values of relative binding affinity (RBA) of PFOS and PFOA to E2 were calculated as 0.014% and 0.0003%. Thus, they are assessed as weak binder (PFOS) and very weak binder (PFOA)

dx.doi.org/10.1021/es304030x | Environ. Sci. Technol. 2013, 47, 634−641

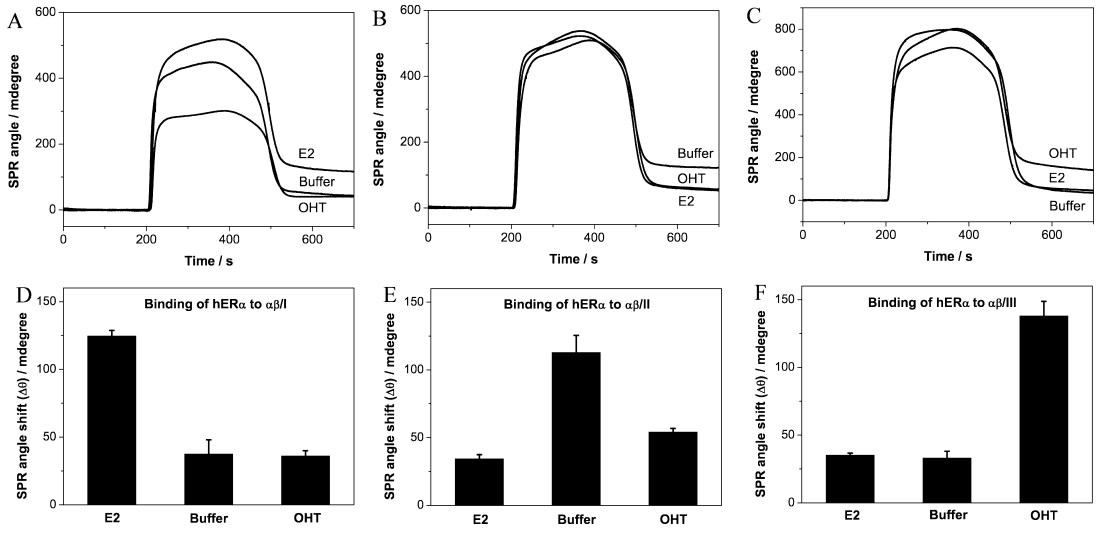

Figure 2. Overlayed sensorgrams and SPR angle shift ($\Delta\theta$) of 50 nM hERα on $\alpha\beta$/I (A, D), $\alpha\beta$/II (B, E) and $\alpha\beta$/III (C, F) peptide modified sensor surfaces after the receptor was incubated separately with buffer, 10 μM E2 and 10 μM OHT.

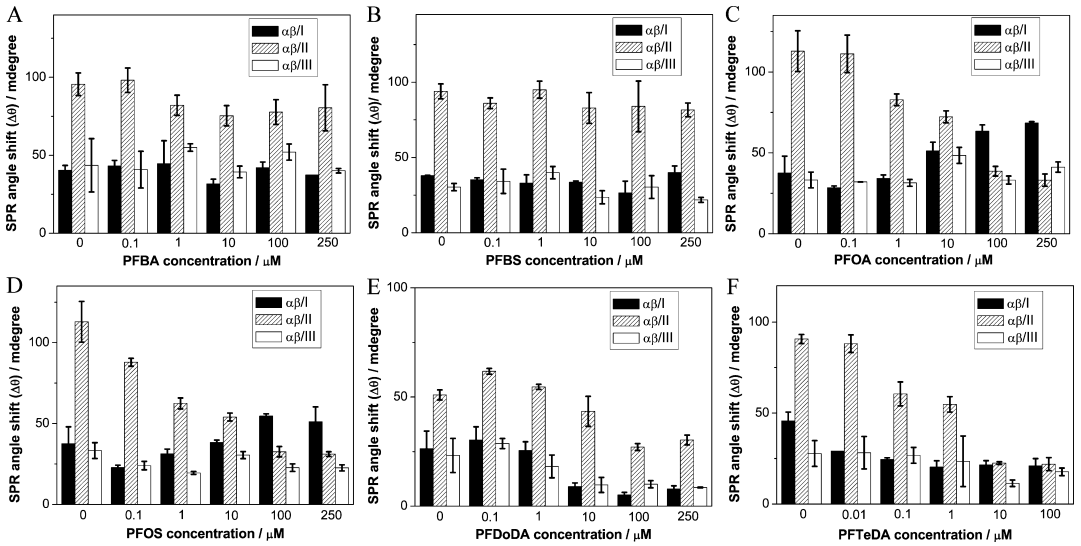

Figure 3. SPR angle shift ($\Delta\theta$) of 50 nM hERα on $\alpha\beta$/I (filled bar), $\alpha\beta$/II (shaded bar) and $\alpha\beta$/III (empty bar) peptide modified sensor surface after the receptor was incubated separately with increasing concentrations of PFBA (A), PFBS (B), PFOA (C), PFOS (D), PFDoDA (E), and PFTeDA (F).

of hERα, respectively. This is in good agreement with the results of a radio-labeled competitive ligand binding assay with trout liver ER.[17] The reason for the different binding affinity with ER among the six PFAAs will be discussed later after computer modeling.

For the measurement of ligand-induced hERα conformational change, a conformation-specific peptide was immobilized on SPR sensor chip through biotin-streptavidin interaction. A mixture of ER and ligand was then passed over the sensor chip. If the ligand binds to ER and induces a conformation state that can be recognized by the peptide, ER will be captured to the surface and generate SPR signal. As shown in SI Figure S2A, injection of 50 nM hERα and 10 μM E2 over $\alpha\beta$/I peptide modified surface produced a 124-millidegree SPR angular shift ($\Delta\theta$) after association and dissociation process. Nonspecific protein binding on the modified surface is very low, as even 1 μM HSA (a serum transport protein) did not generate any significant SPR signal.

Reproducibility is a major issue in the exploration of SPR biosensors. After receptor binding and SPR measurement, the peptide-modified sensor surface was regenerated with an injection of 0.1 M NaOH to remove surface-bound receptor. After regeneration, another measurement could be carried out on the same chip. As can be seen in SI Figure S2B, the SPR binding curve did not change much even after 12 cycles of receptor binding and surface regeneration. This demonstrates the effectiveness of the regeneration procedure. In addition, it seems that the procedure did not cause any degradation to the sensor surface, as a stable baseline in the sensorgram was maintained after five consecutive injections of NaOH (SI Figure S2C).

To validate the selectivity of the SPR biosensor for a particular conformational state of ER, a peptide modified sensor chip was tested by injecting a solution of hERα preincubated with buffer, 10 μM E2, or 10 μM OHT. The sensorgram for each treatment was recorded, and SPR angular shift ($\Delta\theta$) was measured from the sensorgram. The three peptides, $\alpha\beta$/I, $\alpha\beta$/

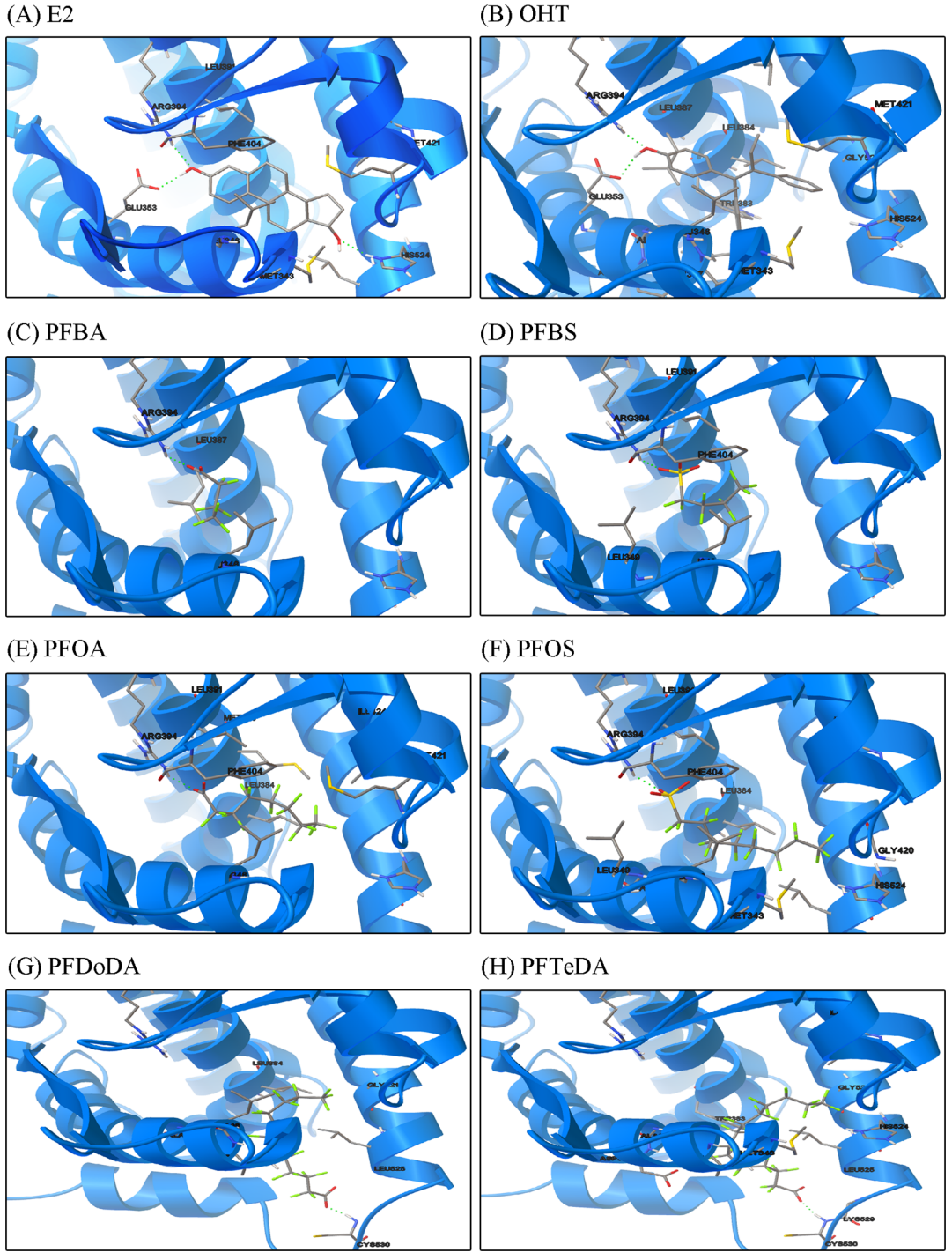

Figure 4. Graphs for the docked complexes between hERα ligand binding domain and E2, OHT and the six PFAAs. The structure with the lowest binding energy for each ligand is shown. The ligands and relevant amino acid residues of the receptor are colored by atom type (carbon in gray, nitrogen in blue, oxygen in red, sulfur in yellow, and fluorine in green). Hydrogen bonds are represented by dotted green lines between the donor and acceptor.

II, and $\alpha\beta$/III, are known to bind selectively to ER with an agonist-induced conformation, inactive conformation, and antagonist-induced conformation, respectively.[24,25] Since E2 is an ER agonist, it is not surprising to find out that the binding of hERα to $\alpha\beta$/I-modified surface is the most when ER was preincubated with E2 (Figure 2). The SPR response is 124 millidegrees, approximately 3 fold higher than the receptor preincubated with buffer or OHT. However, on $\alpha\beta$/II modified surface the buffer-treated hERα binds substantially more than the other two solutions (E2 and OHT). Similarly, on $\alpha\beta$/III modified surface more binding was observed with OHT-treated ER than buffer and E2. All the results described above demonstrate that each peptide surface is selective toward a particular ligand-induced ER conformation state. In a previous work,[25] eight ligands of known ER activity (including estradiol and tamoxifen) were tested by time-resolved fluorescence assays, and good selectivity was obtained with the three conformation-selective peptides. Using our SPR biosensor, the

dx.doi.org/10.1021/es304030x | *Environ. Sci. Technol.* 2013, 47, 634−641

effect of a chemical on human estrogen receptor can be evaluated.

After the biosensor approach was validated, the six selected PFAAs were evaluated for their estrogenic activities. In the experiment, a PFAA of a series of concentrations was preincubated with hERα, and then reacted separately with one of the three peptide sensor chips. The results are shown in Figure 3. Without addition of any PFAA, the SPR signal of the receptor was the highest on $\alpha\beta$/II peptide modified surface. This indicates that, understandably, the receptor was in a rest state. Upon addition of PFBA up to 250 μM, SPR signal on any one of the three peptide surfaces did not significantly change (Figure 3A). With 250 μM PFBA added, SPR intensity was 30, 80, and 30 millidegrees respectively on $\alpha\beta$/I, $\alpha\beta$/II and $\alpha\beta$/III surface, which is almost the same as the value before PFBA addition. Similar results were obtained with PFBS. These peptide binding results alone suggest that the two 4-carbon fluorinated chemicals either did not bind with ER, or they did bind with ER but did not induce any conformation change. However, when combined with the direct ER binding results summarized in Table 1, it can be concluded that PFBA and PFBS do not bind with ER in any appreciable way.

The situation with 8-carbon PFOA and PFOS is quite different. With increasing concentration of PFOA, SPR signal of ER on $\alpha\beta$/II surface decreased progressively, and the signal on $\alpha\beta$/I surface increased accordingly. Meanwhile, the response on $\alpha\beta$/III surface stayed mostly unchanged. At the highest PFOA concentration tested (250 μM), SPR intensity on $\alpha\beta$/I surface became the largest, and is about 2 times as much as the blank. Similar results were obtained with PFOS. The results suggest that PFOA and PFOS bound with hERα and induced the receptor to change from the rest state to the agonist conformation, and that this conformation change is concentration dependent. It should be noted that, even at 250 μM concentration, the $\Delta\theta$ values obtained with PFOA and PFOS on $\alpha\beta$/I surface are only about 1.5−2 fold higher than the blank. However, with as low as 10 μM E2, the increase was 3.3-fold. Therefore, PFOA and PFOS can be considered as weak agonists of hERα.

For longer-chain PFAAs, PFDoDA (12 carbon) and PFTeDA (14 carbon), the $\Delta\theta$ value of hERα on $\alpha\beta$/II surface decreased substantially with increasing PFAA concentration. At the same time, the signal was also reduced, albeit slightly, on the other two peptide surfaces. This was initially very puzzling to us. If the signal reduction observed on the $\alpha\beta$/II surface is due to ER conformation change induced by PFAA binding, ER would change to a conformation which should be detected on either $\alpha\beta$/I or $\alpha\beta$/III surface. However, there is no concomitant signal increase on the latter two peptide surfaces. Therefore, one would begin to suspect that the loss of SPR signal has nothing to do with ER conformation change. Recalling that the direct ER binding measurement revealed that neither PFDoDA nor PFTeDA bound to ER, an alternative explanation was explored. It was later found out that there existed some nonspecific adsorption of PFAAs on the sensor chip surface. As shown in SI Figure S3, 100 μM PFTeDA or PFDoDA alone (without ER) produced a significant SPR signal, whereas the other four PFAAS generated much smaller signal. It is plausible that the nonspecific adsorption of PFDoDA and PFTeDA on the surface might block the binding of ER with the peptide, and therefore lead to SPR signal reduction in Figure 3E,F.

Putting together, the direct ER binding and peptide binding measurements revealed that the six tested PFAAs had different binding affinity with ER, and the two 8-carbon compounds had estrogenic activity. Differences in estrogenic activities among various PFAAs were also observed in previous in vivo and cell assays.[15,17] To understand the structural basis of these differences, molecular modeling on the interactions between PFAAs and hERα was performed. E2 (the endogenous ligand) and OHT (a known ER antagonist) were first docked to hERα-LBD using the Autodock software. The calculations were performed with both rigid and flexible amino acid side chains of the ER binding pocket. We found that the docking results were much more consistent with their crystallographic structures when the calculations were performed with rigid side chains. Hydrogen bond interactions were found between the phenolic hydroxyl group of the A-ring of E2 and the side chain residues of Glu353 (H3) and Arg394 (H6) at one end of the binding cavity in ER, and between the hydroxyl group of the E2 D-ring and His524 (H11) at the other end of the cavity (Figure 4A). For OHT, hydrogen bonds were formed between its phenolic hydroxyl group and Glu353 and Arg394, and the long side chain protruded from the pocket between H3 and H11 (Figure 4B). These modeling results are in good agreement with the crystallographic observations,[22,23] even though water molecules such as the one between Arg394 and Glu353 in the crystal structure were deleted in the docking experiments. Using the same constraints, the six PFAAs were docked with hER-LBD. In the docked complexes with PFOA and PFOS, a hydrogen bond was formed between the carboxylic acid or sulfonate group of the chemical and Arg394 of ER. The fluorinated carbon chains participated in a number of hydrophobic contacts with the closed side chains of the amino acids including Met343, Leu346, Phe404, Met421, and His524, which also exit in the docked E2 complex. Further more, the two 8-carbon PFAAs nestled the whole binding cavity from Glu353 and Arg394 to His524. In general, there are great similarities in the ligand-hERα binding interactions between PFOA, PFOS, and E2. For PFBA and PFBS, the same hydrogen-bonding patterns were found (Arg394), with less hydrophobic interaction due to shorter carbon chains. However, PFDoDA and PFTeDA showed completely different interactions with hERα-LBD by comparison with 4-carbon and 8-carbon PFAAs. Cys530 is the most favored residue to form hydrogen bond with the carboxylic acid group of these two compounds. The docked complexes are expected to be very unstable, because only about half of the molecule resides inside the defined binding pocket for E2.

Based on the molecular docking results, the binding energy between each ligand and hERα-LBD was calculated, and listed in Table 2. The order of binding energy is E2, OHT ≫ PFOS,

Table 2. Molecular Docking of the Interactions between the Selected Ligands and hERα Ligand Binding Domain

ligand	binding energy (kcal/M)	hydrogen-bonding interaction	length of ligand (Å)
E2	−10.39	Arg394, Glu353, His524	11.13
OHT	−11.30	Arg394, Glu353	11.13
PFBA	−1.82	Arg394	6.02
PFBS	−1.99	Arg394	7.15
PFOA	−2.22	Arg394	9.64
PFOS	−2.44	Arg394	11.98
PFDoDA	−0.99	Cys530	14.08
PFTeDA	−1.13	Cys530	18.10

PFOA, PFBA, PFBS > PFDoDA, PFTeDA, with E2 and OHT substantially larger than all other ligands. The binding affinity measured in our SPR experiments follows the order of E2 > OHT ≫ PFOS > PFOA > PFBA, PFBS, PFDoDA, PFTeDA, with E2 × 10^4−10^5 fold stronger than the others. Therefore, there seems to be some correlation between the calculated binding energy and experimentally measured binding affinity, an indication for the goodness of the molecular docking. The difference in ER binding affinity among the six PFAAs can be rationalized by considering the structural differences as revealed in the docked ligand−receptor complexes. First of all, we can consider the match of size between ER binding cavity and a ligand. According to the crystallographic structure, the length of the binding cavity in ER is around 11 Å, spanning from Arg394 and Glu353 to His524. The molecular length of E2 and OHT is 11.127 Å and 11.129 Å, respectively, which matches well with the binding cavity. The molecular length of PFBA, PFBS, PFOS, and PFOA is 6.025 Å, 7.152 Å, 11.979 Å, and 9.645 Å respectively, and they can all fit into the cavity. With 14.080 Å and 18.105 Å in length, PFDoDA and PFTeDA are too long to be confined inside the binding cavity without any strong torsion. Second, we can consider the number of hydrogen bonds formed and extent of hydrophobic contact in the ligand−receptor complex. For E2, three hydrogen bonds are formed, involving Arg394, Glu353, and His524. However, even though the 4-carbon and 8-carbon PFAAs can fit into the binding cavity, only one hydrogen bond with Arg394 is formed. This explains why these chemicals have much lower binding affinity for ER than E2. The 4-carbon PFAAs are further compromised by having less hydrophobic interactions in the binding cavity than the 8-carbon PFAAs. Overall, PFOA and PFOS have the right structure to possess the strongest binding affinity for ER among the six PFAAs.

We can now consider the effect of PFAA binding on ER conformation. Our SPR peptide binding measurements revealed that PFOS and PFOA bound with ER and induced the receptor to an agonist conformation, which suggest that the two PFAAs have estrogenic activities. In a previous study using trans-activation assays with hERα in HEK-293T cells, 8−10 carbon perfluoroalkyl acids induced gene reporter activity up to 2.5-fold at concentrations of 100−1000 nM, and PFOS was the most effective exoestrogen of the tested PFAAs.[17] Therefore, PFOA- and PFOS-induced ER conformation change appears to correlate with their biological effects in human cells. In the docked E2-ER complex, there exist three hydrogen bonds with Arg394, Glu353, and His524. However, in the docked FPFOS- or PFOA-ER complex, only one hydrogen bond with Arg394 was formed. Yet the two chemicals still activated ER conformation and exhibited estrogenic activities in cells. It can therefore be postulated that Arg394 is the most critical amino acid involved in the binding of an agonist with ER and subsequent change of ER conformation.

To conclude, we have developed a SPR-based peptide biosensor which can discriminate between agonists and antagonists of hERα by monitoring the conformation change of the receptor induced by ligand binding. This biosensor is highly conformation-selective and reproducible, and can be used as a rapid screening tool for the assessment of estrogenic activity of chemicals. Six PFAAs of various chain length and acid groups were tested with the biosensor. Two 8-carbon PFAAs, PFOS, and PFOA, were found to bind weakly to hERα and induce the receptor to an agonist conformation in a concentration-dependent manner. Molecular docking revealed that the size of the two PFAAs and their hydrogen bonding with Arg-394 are the important structural characteristics for them to act as ER agonists. Our work suggests that the combination of mechanism-based analytical method and computer modeling can offer some unique insight into the molecular toxicology and mode of action of industrial and environmental chemicals. The approach is rapid and cost-effective, and can be used to complement animal tests and cell assays.

■ ASSOCIATED CONTENT

Supporting Information

Structures of E2, OHT, and the six selected PFAAs, SPR peptide sensor evaluation, and SPR sensorgrams of nonspecific adsorption of the six PFAAs (100 μM) on $\alpha\beta$/II peptide modified sensor surface. This material is available free of charge via the Internet at http://pubs.acs.org.

■ AUTHOR INFORMATION

Corresponding Author

*Phone/fax: (86)-10-62849685; e-mail: LHGuo@rcees.ac.cn.

Notes

The authors declare no competing financial interest.

■ ACKNOWLEDGMENTS

This work was financially supported by the National Natural Science Foundation of China (20890112, 20825519, 20921603) and the Ministry of Science and Technology of China (2010DFA92090).

■ REFERENCES

(1) 3M Company. *Environmental and Health Assessment of Perfluorooctanesulfonate and Its Salts*; US EPA Administrative Record AR-226−1486; U.S. Environmental Protection Agency: Washington, DC, 2003.

(2) Giesy, J. P.; Kannan, K. Perfluorochemical surfactants in the environment. *Environ. Sci. Technol.* **2002**, *36* (7), 146A−152A.

(3) Houde, M.; Martin, J. W.; Letcher, R. J.; Solomon, K. R.; Muir, D. C. G. Biological monitoring of polyfluoroalkyl substances: A review. *Environ. Sci. Technol.* **2006**, *40* (11), 3463−3473.

(4) Giesy, J. P.; Kannan, K. Global distribution of perfluorooctane sulfonate in wildlife. *Environ. Sci. Technol.* **2001**, *35* (7), 1339−1342.

(5) Kennedy, G. L.; Butenhoff, J. L.; Olsen, G. W.; O'Connor, J. C.; Seacat, A. M.; Perkins, R. G.; Biegel, L. B.; Murphy, S. R.; Farrar, D. G. The toxicology of perfluorooctanoate. *Crit. Rev. Toxicol.* **2004**, *34* (4), 351−384.

(6) Conder, J. M.; Hoke, R. A.; De Wolf, W.; Russell, M. H.; Buck, R. C. Are PFCAs bioaccumulative? A critical review and comparison with regulatory lipophilic compounds. *Environ. Sci. Technol.* **2008**, *42* (4), 995−1003.

(7) Lau, C.; Anitole, K.; Hodes, C.; Lai, D.; Pfahles-Hutchens, A.; Seed, J. Perfluoroalkyl acids: A review of monitoring and toxicological findings. *Toxicol. Sci.* **2007**, *99* (2), 366−394.

(8) Andersen, M. E.; Butenhoff, J. L.; Chang, S. C.; Farrar, D. G.; Kennedy, G. L.; Lau, C.; Olsen, G. W.; Seed, J.; Wallace, K. B. Perfluoroalkyl acids and related chemistries—Toxicokinetics and modes of action. *Toxicol. Sci.* **2008**, *102* (1), 3−14.

(9) DeWitt, D. E.; Shnyra, A.; Badr, M. Z.; Loveless, S. E.; Hoban, D.; Frame, S. R.; Cunard, R.; Anderson, S. E.; Meade, B. J.; Peden-Adams, M. M.; Luebke, R. W.; Luster, M. I. Immunotoxicity of perfluorooctanoic acid and perfluorooctane sulfonate and the role of peroxisome proliferator-activated receptor alpha. *Crit. Rev. Toxicol.* **2009**, *39* (1), 76−94.

(10) Chen, Y.-M.; Guo, L.-H. Fluorescence study on site-specific binding of perfluoroalkyl acids to human serum albumin. *Arch. Toxicol.* **2008**, *83* (3), 255−261.
(11) Hebert, P. C.; MacManus-Spencer, L. A. Development of a fluorescence model for the binding of medium- to long-chain perfluoroalkyl acids to human serum albumin through a mechanistic evaluation of spectroscopic evidence. *Anal. Chem.* **2010**, *82* (15), 6463−6471.
(12) Ito, Y.; Yamanoshita, O.; Asaeda, N.; Tagawa, Y.; Lee, C. H.; Aoyama, T.; Ichihara, G.; Furuhashi, K.; Kamijima, M.; Gonzalez, F. J.; Nakajima, T. Di(2-ethylhexyl)phthalate induces hepatic tumorigenesis through a peroxisome proliferator-activated receptor alpha-independent pathway. *J. Occup. Health* **2007**, *49* (3), 172−182.
(13) Caldwell, J. C.; Brown, R. C.; Siegel Scott, C.; Jinot, J.; Bateson, T. F.; Chiu, W. A.; Guyton, K. Z. A reexamination of the PPAR-α activation mode of action as a basis for assessing human cancer risks of environmental contaminants. *Environ. Health Perspect.* **2009**.
(14) Tilton, S. C.; Orner, G. A.; Benninghoff, A. D.; Carpenter, H. M.; Hendricks, J. D.; Pereira, C. B.; Williams, D. E. Genomic profiling reveals an alternate mechanism for hepatic tumor promotion by perfluorooctanoic acid in rainbow trout. *Environ. Health Perspect.* **2008**, *116* (8), 1047−1055.
(15) Liu, C.; Du, Y.; Zhou, B. Evaluation of estrogenic activities and mechanism of action of perfluorinated chemicals determined by vitellogenin induction in primary cultured tilapia hepatocytes. *Aquat. Toxicol.* **2007**, *85* (4), 267−277.
(16) Ishibashi, H.; Yamauchi, R.; Matsuoka, M.; Kim, J.-W.; Hirano, M.; Yamaguchi, A.; Tominaga, N.; Arizono, K. Fluorotelomer alcohols induce hepatic vitellogenin through activation of the estrogen receptor in male medaka (*Oryzias latipes*). *Chemosphere* **2008**, *71* (10), 1853−1859.
(17) Benninghoff, A. D.; Bisson, W. H.; Koch, D. C.; Ehresman, D. J.; Kolluri, S. K.; Williams, D. E. Estrogen-like activity of perfluoroalkyl acids in vivo and interaction with human and rainbow trout estrogen receptors in vitro. *Toxicol. Sci.* **2011**, *120* (1), 42−58.
(18) Thibodeaux, J. R.; Hanson, R. G.; Rogers, J. M.; Grey, B. E.; Barbee, B. D.; Richards, J. H.; Butenhoff, J. L.; Stevenson, L. A.; Lau, C. Exposure to perfluorooctane sulfonate during pregnancy in rat and mouse. I: Maternal and prenatal evaluations. *Toxicol. Sci.* **2003**, *74* (2), 369−381.
(19) Lau, C.; Thibodeaux, J. R.; Hanson, R. G.; Rogers, J. M.; Grey, B. E.; Stanton, M. E.; Butenhoff, J. L.; Stevenson, L. A. Exposure to perfluorooctane sulfonate during pregnancy in rat and mouse. II: Postnatal evaluation. *Toxicol. Sci.* **2003**, *74* (2), 382−392.
(20) Chang, S. C.; Thibodeaux, J. R.; Eastvold, M. L.; Ehresman, D. J.; Bjork, J. A.; Froehlich, J. W.; Lau, C. S.; Singh, R. J.; Wallace, K. B.; Butenhoff, J. L. Negative bias from analog methods used in the analysis of free thyroxine in rat serum containing perfluorooctanesulfonate (PFOS). *Toxicology* **2007**, *234* (1−2), 21−33.
(21) Heldring, N.; Pike, A.; Andersson, S.; Matthews, J.; Cheng, G.; Hartman, J.; Tujague, M.; Strom, A.; Treuter, E.; Warner, M.; Gustafsson, J. A. Estrogen receptors: How do they signal and what are their targets. *Physiol. Rev.* **2007**, *87* (3), 905−931.
(22) Brzozowski, A. M.; Pike, A. C. W.; Dauter, Z.; Hubbard, R. E.; Bonn, T.; Engstrom, O.; Ohman, L.; Greene, G. L.; Gustafsson, J. A.; Carlquist, M. Molecular basis of agonism and antagonism in the oestrogen receptor. *Nature* **1997**, *389* (6652), 753−758.
(23) Shiau, A. K.; Barstad, D.; Loria, P. M.; Cheng, L.; Kushner, P. J.; Agard, D. A.; Greene, G. L. The structural basis of estrogen receptor/coactivator recognition and the antagonism of this interaction by tamoxifen. *Cell* **1998**, *95* (7), 927−937.
(24) Norris, J. D.; Paige, L. A.; Christensen, D. J.; Chang, C. Y.; Huacani, M. R.; Fan, D. J.; Hamilton, P. T.; Fowlkes, D. M.; McDonnell, D. P. Peptide antagonists of the human estrogen receptor. *Science* **1999**, *285* (5428), 744−746.
(25) Paige, L. A.; Christensen, D. J.; Gron, H.; Norris, J. D.; Gottlin, E. B.; Padilla, K. M.; Chang, C. Y.; Ballas, L. M.; Hamilton, P. T.; McDonnell, D. P.; Fowlkes, D. M. Estrogen receptor (ER) modulators each induce distinct conformational changes in ER alpha and ER beta. *Proc. Natl. Acad. Sci. U. S. A.* **1999**, *96* (7), 3999−4004.
(26) Mukhopadhyay, R.; Sumbayev, V. V.; Lorentzen, M.; Kjems, J.; Andreasen, P. A.; Besenbacher, F. Cantilever sensor for nano-mechanical detection of specific protein conformations. *Nano Lett.* **2005**, *5* (12), 2385−2388.
(27) Hansen, J. A.; Surnbayev, V. V.; Gothelf, K. V. An electrochemical sensor based on the human estrogen receptor ligand binding domain. *Nano Lett.* **2007**, *7* (9), 2831−2834.
(28) Fechner, P.; Proll, F.; Carlquist, M.; Proll, G. An advanced biosensor for the prediction of estrogenic effects of endocrine-disrupting chemicals on the estrogen receptor alpha. *Anal. Bioanal. Chem.* **2009**, *393* (6−7), 1579−1585.
(29) Homola, J. Surface plasmon resonance sensors for detection of chemical and biological species. *Chem. Rev.* **2008**, *108* (2), 462−493.
(30) Rich, R. L.; Hoth, L. R.; Geoghegan, K. F.; Brown, T. A.; LeMotte, P. K.; Simons, S. P.; Hensley, P.; Myszka, D. G. Kinetic analysis of estrogen receptor/ligand interactions. *Proc. Natl. Acad. Sci. U. S. A.* **2002**, *99* (13), 8562−8567.
(31) Morris, G. M.; Goodsell, D. S.; Halliday, R. S.; Huey, R.; Hart, W. E.; Belew, R. K.; Olson, A. J. Automated docking using a Lamarckian genetic algorithm and an empirical binding free energy function. *J. Comput. Chem.* **1998**, *19* (14), 1639−1662.
(32) Morris, G. M.; Huey, R.; Lindstrom, W.; Sanner, M. F.; Belew, R. K.; Goodsell, D. S.; Olson, A. J. AutoDock4 and AutoDockTools4: Automated docking with selective receptor flexibility. *J. Comput. Chem.* **2009**, *30* (16), 2785−2791.
(33) Bolger, R.; Wiese, T. E.; Ervin, K.; Nestich, S.; Checovich, W. Rapid screening of environmental chemicals for estrogen receptor binding capacity. *Environ. Health Perspect.* **1998**, *106* (9), 551−557.
(34) Gangloff, M.; Ruff, M.; Eiler, S.; Duclaud, S.; Wurtz, J. M.; Moras, D. Crystal structure of a mutant hER alpha ligand-binding domain reveals key structural features for the mechanism of partial agonism. *J. Biol. Chem.* **2001**, *276* (18), 15059−15065.
(35) Kuiper, G.; Carlsson, B.; Grandien, K.; Enmark, E.; Haggblad, J.; Nilsson, S.; Gustafsson, J. A. Comparison of the ligand binding specificity and transcript tissue distribution of estrogen receptors alpha and beta. *Endocrinology* **1997**, *138* (3), 863−870.
(36) Sun, J.; Meyers, M. J.; Fink, B. E.; Rajendran, R.; Katzenellenbogen, J. A.; Katzenellenbogen, B. S. Novel ligands that function as selective estrogens or antiestrogens for estrogen receptor-alpha or estrogen receptor-beta. *Endocrinology* **1999**, *140* (2), 800−804.
(37) Labrie, F.; Labrie, C.; Belanger, A.; Simard, J.; Gauthier, S.; Luu-The, V.; Merand, Y.; Giguere, V.; Candas, B.; Luo, S. Q.; Martel, C.; Singh, S. M.; Fournier, M.; Coquet, A.; Richard, V.; Charbonneau, R.; Charpenet, G.; Tremblay, A.; Tremblay, G.; Cusan, L.; Veilleux, R. EM-652 (SCH 57068), a third generation SERM acting as pure antiestrogen in the mammary gland and endometrium. *J. Steroid Biochem. Mol. Biol.* **1999**, *69* (1−6), 51−84.